

See discussions, stats, and author profiles for this publication at: <https://www.researchgate.net/publication/264982120>


# Topology optimization of compliant mechanisms with desired structural stiffness

**Article** in *Engineering Structures* · November 2014  
DOI: 10.1016/j.engstruct.2014.08.008

CITATIONS  
13


READS  
1,079

4 authors, including:



**X. Huang**  
Swinburne University of Technology  
**164** PUBLICATIONS **2,553** CITATIONS


SEE PROFILE




**Yi Min Xie**  
RMIT University  
**316** PUBLICATIONS **7,422** CITATIONS

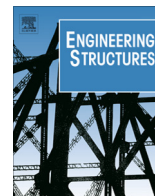
SEE PROFILE

Some of the authors of this publication are also working on these related projects:

- 

Developing advanced materials and structures based on the concept of topological interlocking [View project](#)
- 

Scientific appraisal for acupuncture from the perspective of needle tool [View project](#)



# Topology optimization of compliant mechanisms with desired structural stiffness



X. Huang<sup>\*</sup>, Y. Li, S.W. Zhou, Y.M. Xie

Centre for Innovative Structures and Materials, School of Civil, Environmental and Chemical Engineering, RMIT University, GPO Box 2476, Melbourne, VIC 3001, Australia

## ARTICLE INFO

### Article history:

Received 13 November 2013

Revised 28 July 2014

Accepted 5 August 2014

### Keywords:

Topology optimization  
Bi-directional evolutionary structural optimization (BESO)  
Compliant mechanisms  
Mean compliance

## ABSTRACT

This paper develops a bi-directional evolutionary structural optimization (BESO) method for topological design of compliant mechanisms. The design problem is reformulated as maximizing the flexibility of the compliant mechanism subject to the mean compliance and volume constraints. Based on the finite element analysis, a new BESO algorithm is established for solving such an optimization problem by gradually updating design variables until a convergent solution is obtained. Several 2D and 3D examples are presented to demonstrate the effectiveness of the proposed BESO method. A series of optimized mechanism designs with or without hinge regions are obtained. Numerical results also indicate that the flexibility and hinge-related property of the optimized compliant mechanisms can be controlled by the desired structural stiffness.

© 2014 Elsevier Ltd. All rights reserved.

## 1. Introduction

Compliant mechanisms are usually monolithic structures that transfer an input force or displacement to another point through elastic deformation. Different from the rigid-link mechanisms, the motions of compliant mechanisms are derived mainly from the relative flexibility of their components. Such monolithic mechanical devices have numerous virtues such as saving space, reducing fatigue and high stress concentration and without any assembly cost [1]. Therefore, the application of compliant mechanisms has become increasingly prevalent in medical instruments and micro-electro-mechanical systems (MEMS). In spite of various advantages in their application, it is challenging to design a compliant mechanism with desired functions. Generally, there are two main approaches to the design of compliant mechanisms, namely the kinematics-based approach [1,2] and the topology optimization-based approach [3–6].

Topology optimization enables designers to find a suitable structural layout for the required performance. It has attracted considerable attention over the past decades and many different techniques such as the homogenization method [7], Solid Isotropic Material with Penalization (SIMP) method [8–10], level-set method [11,12] and evolutionary structural optimization (ESO) method [13,14] and others [15–17] have been developed. The ESO method is based on a simple concept that inefficient material

is gradually removed from the design domain so that the resulting topology evolves toward an optimum. The later version of the ESO method, namely bi-directional ESO (BESO), allows not only to remove elements from the least efficient regions, but also to add elements in the most efficient regions simultaneously [18–20]. It has been demonstrated that the current BESO method is capable of generating reliable and practical topologies for optimization problems with various constraints such as stiffness [21], frequency [22] or energy absorption [23–25].

The design of compliant mechanisms using topology optimization techniques has been exhaustively explored in previous decades [3–6]. Generally, an efficient compliant mechanism as shown in Fig. 1(a) should be flexible enough to produce the expected kinematic motion (flexibility) but should also be stiff enough to resist external forces (stiffness). The flexibility and stiffness characters of a compliant mechanism can be quantified using relationships between the applied forces, the resulting displacements at the input port of the mechanism, and the resulting displacements and reaction forces at the output port of the mechanism. The topology optimization problem has been formulated in a number of alternative ways through utilization of assorted objective and constraint functions due to the inherent multi-objective performance demand. The objective function can be defined by the output displacement, geometric advantage (GA, the ratio of input and output displacements) or mechanical advantage (MA, the ratio of input and output forces) [5,6,26–28] according to the flexibility function of the compliant mechanism. Alternatively, the mutual potential energy (MPE), the strain energy

<sup>\*</sup> Corresponding author. Tel.: +61 3 99253320; fax: +61 3 96390138.

E-mail address: [huang.xiaodong@rmit.edu.au](mailto:huang.xiaodong@rmit.edu.au) (X. Huang).

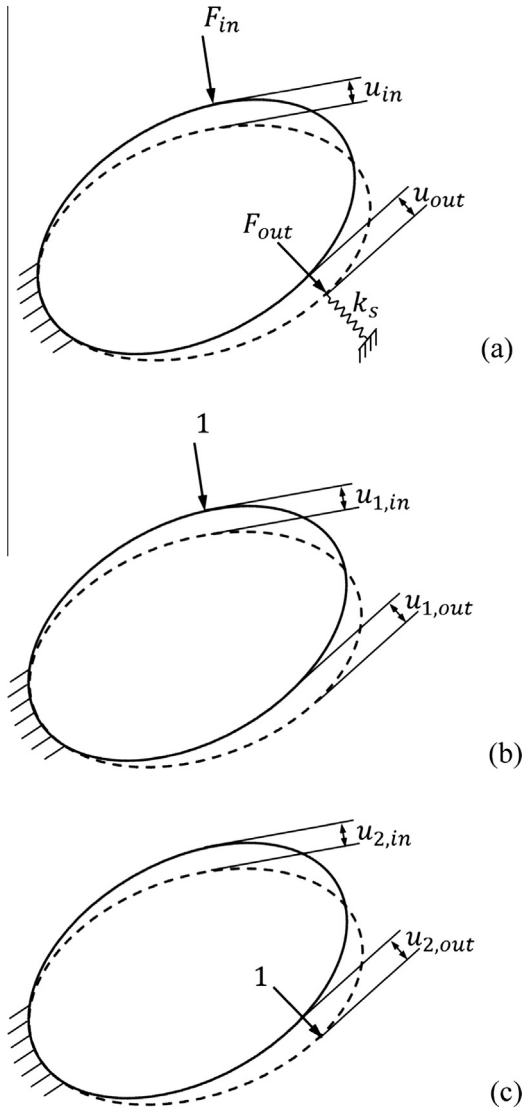


Fig. 1. (a) Compliant mechanism; (b) input unit dummy load case; (c) output unit dummy load case.

(SE) or other equivalent measurements can be used as a single or multiple objective functions to qualify the combination of structural flexibility and stiffness [4,29–33].

Designing compliant mechanisms using topology optimization methods typically results in *de facto* hinge regions in the design models due to the problem formulation. The existence of *de facto* hinge regions makes compliant mechanisms function as rigid-link mechanisms so as to maximize their capability of transferring kinematic motion. Due to the difficulties in manufacturing reliable hinges especially for micro-scale mechanical systems, designing monolithic and hinge-free compliant mechanisms has attracted extensively attention and undergone considerable development in recent years. Rahmatalla and Swan [30] conducted an review on a number of different techniques for eliminating *de facto* hinges in the design of compliant mechanisms. The topology optimization formulation by imbedding wavelet base functions was developed to preclude the formation of *de facto* hinge regions [34,35]. Other approaches attempted to eliminate *de facto* hinge regions include imposing a minimum length constraint [36] or filter schemes [37]. Such morphology-based approaches could greatly reduce the occurrence of one-node connected hinges, but were not entirely effective due to the nature of the optimization problem. Reformulating the problem as a multi-criteria optimization might

be an effective way for entirely circumventing *de facto* hinge regions which generally lie along the force path from the mechanism input port to the output port. For example, simultaneously maximizing the flexibility and minimizing the stiffness of the input-restrained structure can achieve hinge-free compliant mechanisms [30,38], and the resulting compliant mechanisms are also stiff and can resist the additional load exerted by the work-piece once it has been secured. Recently, Zhu et al. [39] incorporated this approach to optimize hinge-free compliant mechanisms with multiple outputs. Nevertheless, it should be noted that the stiffness of a compliant mechanism is only equivalent to that of the input-restrained structure when the stiffness of the work-piece tends to infinity.

With a given stiffness of the work-piece, the formation of *de facto* hinge regions must be correlated with the structural stiffness of compliant mechanisms. This paper proposes a new BESO method for optimally designing the flexibility of compliant mechanisms by altering the desired structural stiffness which includes the influence of external loads exerted by the work-piece. The paper is organized as follows: Section 2 reformulates the optimization problem of compliant mechanisms and derives the sensitivities of objective and constraint functions. Section 3 describes the BESO algorithm and its numerical implementation. Section 4 presents numerical examples and discusses the formulation of *de facto* hinge regions. Concluding remarks are made in Section 5.

## 2. Problem formulation for the design of compliant mechanism

Consider the design domain of a compliant mechanism where  $F_{in}$  is the applied force at the input port and  $u_{out}$  is the expected output displacement at the output port as shown in Fig. 1a. A spring with a constant stiffness,  $k_s$ , is introduced to simulate the interaction between the work-piece and the compliant mechanism.  $u_{in}$  is the resulting displacement at the input port and  $F_{out} = k_s u_{out}$  is the output force.

When the mechanism behaves in a linear elastic fashion, the displacement field of the mechanism can be calculated according to the displacements caused by the input unit dummy load case (Fig. 1b) and the output unit dummy load case (Fig. 1c).  $u_{1,in}$  and  $u_{1,out}$  denote the displacements at the input port and the output port of the input unit dummy load case. Similarly,  $u_{2,in}$  and  $u_{2,out}$  denote the displacements at the input port and the output port of the output unit dummy load case. Thus, the displacements  $u_{in}$  and  $u_{out}$  at the input and output ports of the mechanism can be found through the superposition of the input unit dummy load case and the output unit dummy load case as

$$u_{in} = F_{in} u_{1,in} - F_{out} u_{2,in} \quad (1)$$

$$u_{out} = F_{in} u_{1,out} - F_{out} u_{2,out} \quad (2)$$

With the relationship of  $F_{out} = k_s u_{out}$ ,  $u_{in}$  and  $u_{out}$  can be explicitly expressed by

$$u_{in} = F_{in} \left( u_{1,in} - \frac{k_s u_{2,in} u_{1,out}}{1 + k_s u_{2,out}} \right) \quad (3)$$

$$u_{out} = \frac{F_{in} u_{1,out}}{1 + k_s u_{2,out}} \quad (4)$$

Generally, compliant mechanisms should efficiently convert applied force or energy at the input port into desired force or energy at the output port. Within a topology optimization framework, a variety of objective functions are defined to find a compliant mechanism with the desired performance [3–6,21–28]. Basically, the performance of compliant mechanisms can be measured by the characteristics of their flexibility and structural

stiffness. The flexibility of a compliant mechanism can be quantified by the resulting displacement at the output port,  $u_{out}$ , which reflects the force/motion transmission ability of compliant mechanisms. While the structural stiffness or mean compliance is one of key factors that must be taken into account in the design of structures. The mean compliance of the compliant mechanism,  $C$ , can be defined as the work done by external forces as

$$C = \frac{1}{2}f_{in}u_{in} - \frac{1}{2}f_{out}u_{out} = \frac{1}{2}f_{in}u_{in} - k_s u_{out}^2 \quad (5)$$

It can be seen that the mean compliance considers the influence of the stiffness of the work-piece which exerts external forces to the compliant mechanism. It should be noted that the definition of the above mean compliance is different from the standard mean compliance which is simply  $f_{in}u_{in}$  [33] or the input-restrained compliance [30].

Instead of using the combination of the flexibility and stiffness as a single objective function [30,32,38] or multiple objective functions [26,33], we reformulate the design of a compliant mechanism by maximizing the output displacement at the output port, and constraining its mean compliance and the amount of structural material that can be used. Mathematically, the optimization problem of a compliant mechanism is expressed by

$$\text{Maximize: } f(x_i) = u_{out} \quad (6)$$

$$\text{Subject to: } C(x_i) \leq C^* \text{ and } V(x_i) = V^* \quad (7)$$

where  $C^*$  and  $V^*$  are the prescribed mean compliance and volume of the compliant mechanism, respectively. The design domain is discretized with finite elements and the volumetric density of each element,  $x_i$ , is used as the design variable. The design variable,  $x_i$ , assumes a value in the interval  $[x_{min}, 1]$  where a small value of  $x_{min}$  e.g. 0.001 represents void and 1 denotes solid. Using the SIMP model [10], the material property of each element is expressed by

$$E(x_i) = x_i^p E^0 \quad (8)$$

where  $E^0$  denotes the Young's modulus of the solid material and  $p$  is the penalty exponent. In numerical examples of this study,  $p = 3$  is used.

To implement BESO based topology optimization technique, sensitivity analysis is necessary for guiding the search direction of the optimization algorithm. Here, both output displacement and mean compliance can be expressed in terms of displacements  $u_{1,in}$ ,  $u_{1,out}$ ,  $u_{2,in}$  and  $u_{2,out}$ . With the help of the material interpolation scheme shown in Eq. (8), the sensitivities of these displacements can be easily derived by using the adjoint method [40].

$$\frac{du_{1,in}}{dx_i} = -px_i^{p-1}\{u_1\}^T [K_i^0]\{u_1\} \quad (9)$$

$$\frac{du_{1,out}}{dx_i} = -px_i^{p-1}\{u_2\}^T [K_i^0]\{u_1\} \quad (10)$$

$$\frac{du_{2,in}}{dx_i} = -px_i^{p-1}\{u_1\}^T [K_i^0]\{u_2\} \quad (11)$$

$$\frac{du_{2,out}}{dx_i} = -px_i^{p-1}\{u_2\}^T [K_i^0]\{u_2\} \quad (12)$$

where  $[K_i^0]$  denotes the elemental stiffness matrix of solid.  $\{u_1\}$  and  $\{u_2\}$  are the displacement fields of the input unit dummy load case and the output unit dummy load case respectively. As a result, the sensitivities of the output displacement and mean compliance can be easily calculated according to Eqs. (4) and (5).

### 3. BESO algorithm

In order to satisfy the compliance constraint, it is necessary to modify the original objective function by adding the constraint through the introduction of a Lagrange multiplier  $\lambda$  [41]. The modified objective function is expressed by

$$\text{Maximize: } f_1(x_i) = u_{out} + \lambda(C^* - C) \quad (13)$$

It can be seen that the modified objective function is equivalent to the original one if the mean compliance is equal to its prescribed value. Otherwise  $\lambda = 0$  if  $C < C^*$  which means the compliance constraint is already satisfied, and  $\lambda$  equals to a certain value if  $C > C^*$  which means we should minimize the mean compliance (or maximize  $-C$ ) to satisfy the constraint in the later iterations. Therefore, the Lagrange multiplier is employed to design compliant mechanisms with the compromise between maximizing  $u_{out}$  and minimizing  $C$  so as to satisfy the compliance constraint.

For the numerical implementation, the objective function can be further modified by

$$\text{Maximize: } f_2(x_i) = wu_{out} + (1 - w)(C^* - C) \quad (14)$$

where  $w$  is a constant ranging from 0 to 1 which will be determined according to the compliance constraint. Thus, it is necessary to estimate the variation of the mean compliance due to the variation of design variables. Based on the value of the mean compliance in the current iteration  $C^k$ , the mean compliance in the next iteration  $C^{k+1}$  can be approximately estimated by

$$C^{k+1} = C^k + \sum_{i=1}^N \frac{dC}{dx_i} \Delta x_i \quad (15)$$

where  $k$  represents the current iteration number and  $N$  is the total number of elements in the design domain. Then, the value of  $w$  can be determined by using a bi-section method in such a way that the compliance constraint will be satisfied in the subsequent iteration [41].

Different from other topology optimization methods, the design variable,  $x_i$ , in the BESO method is of discrete values. In each iteration, the variation of the design variable is a constant,  $\Delta x_i$ . In the traditional BESO method,  $\Delta x_i = 1$  means that elements can only be solid or void [19]. In this paper,  $\Delta x_i = 0.02$  is used which means that there are a number of intermediate values other than  $x_{min}$  and 1 for design variables. Numerical examples will demonstrate that *de facto* hinge regions in compliant mechanisms can be stably formed due to the existence of these intermediate values of the design variable.

BESO starts from the initial full design and gradually decreases or increase the value of  $x_i$  with  $\Delta x_i$  in each iteration. The total volume of the compliant mechanism gradually decreases until the objective volume is achieved, and the volume for the next iteration is calculated by

$$V^{k+1} = \min(V^k(1 - ER), V^*) \quad (16)$$

where  $ER$  is evolution rate such as 1%. Then, the variation of the design variables will be determined according to the relative ranking of sensitivity numbers and the sensitivity number of the  $i$ th element is expressed by

$$\alpha_i = \frac{df_2(x_i)}{dx_i} \quad (17)$$

In addition, the filtering scheme can effectively alleviate the numerical instabilities of the checkerboard pattern and mesh-dependency in the BESO method [19]. The modified sensitivity number of the  $i$ th element is

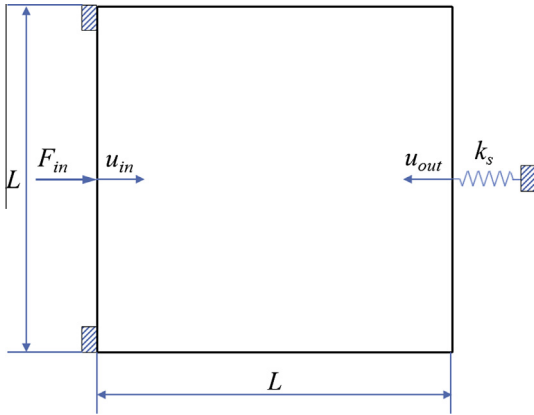


Fig. 2. Design domain and boundary conditions of the compliant inverter.

$$\tilde{\alpha}_i = \frac{\sum_{j=1}^N w_{ij} \alpha_j}{\sum_{j=1}^N w_{ij}} \quad (18)$$

where the weight factor  $w_{ij}$  is defined by

$$w_{ij} = \begin{cases} r_{\min} - r_{ij} & \text{if } r_{ij} < r_{\min} \\ 0 & \text{otherwise} \end{cases} \quad (19)$$

Here,  $r_{ij}$  denotes the distance between the centers of elements  $i$  and  $j$ . The filter radius,  $r_{\min}$  is defined to identify the neighboring elements that affect the sensitivity number of element  $i$ . To improve the convergence of the solution, elemental sensitivity numbers can be further averaged with their corresponding values in the previous iteration as [19]

$$\hat{\alpha}_i = \frac{1}{2} (\tilde{\alpha}_i^k + \tilde{\alpha}_i^{k-1}) \quad (20)$$

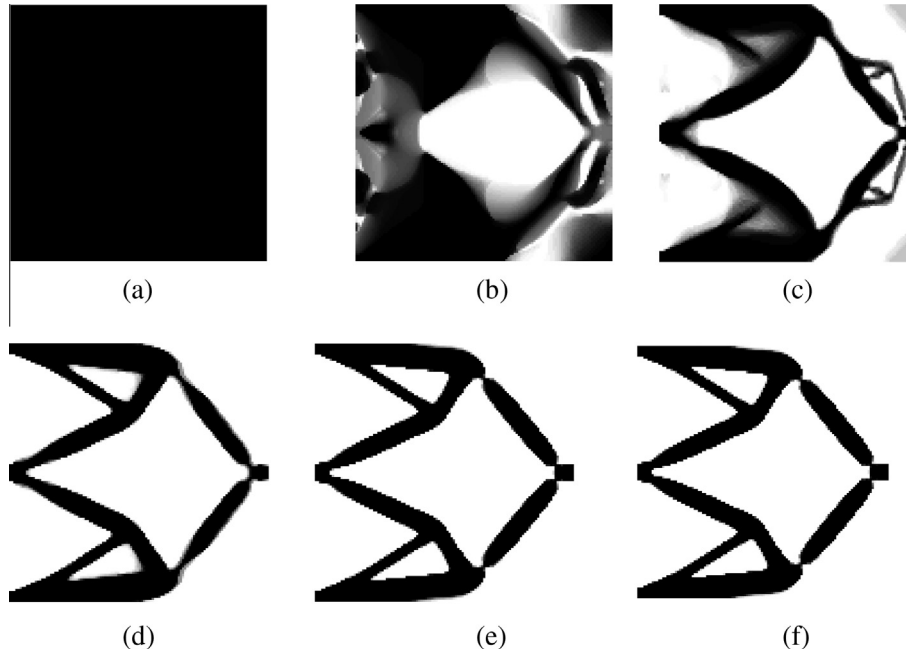


Fig. 3. Evolution history of the topology (a) initial design; (b) 50 iteration; (c) 100 iteration; (d) 150 iteration; (e) 200 iteration; (f) final design.

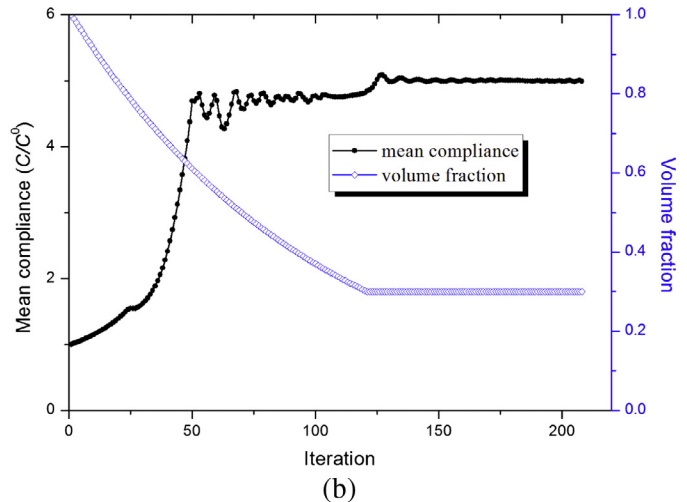
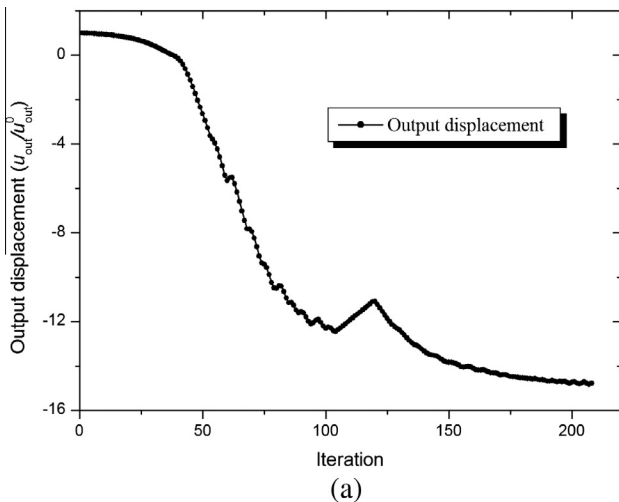
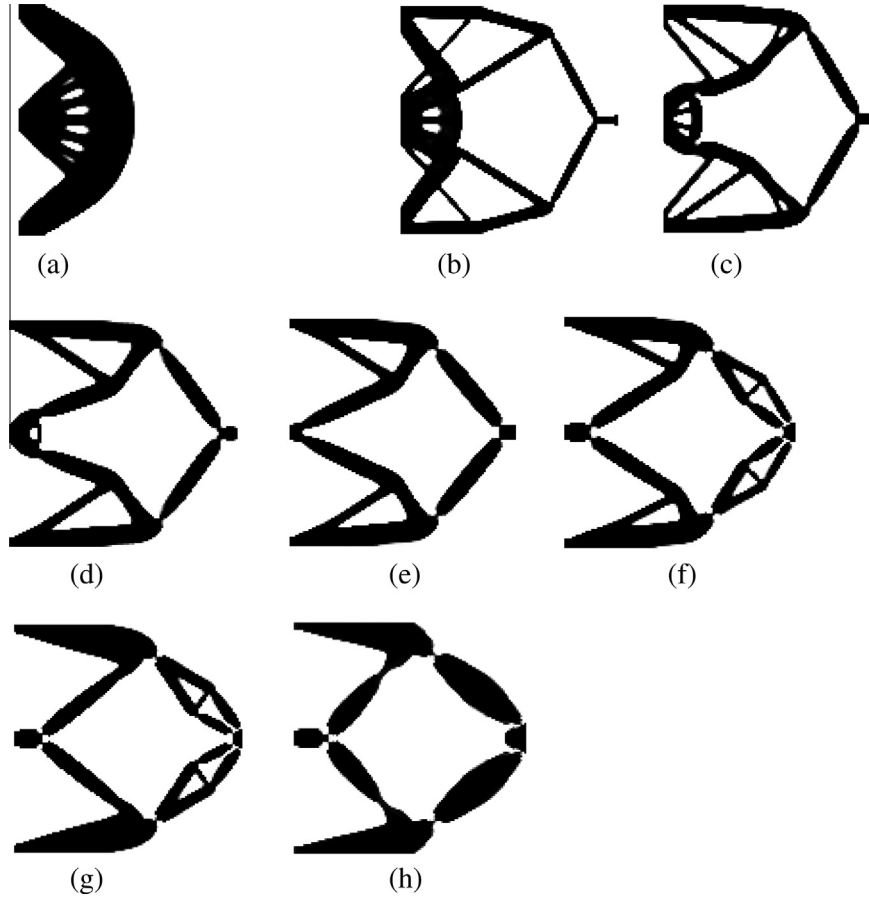


Fig. 4. Evolution histories of the objective function and constraints (a) evolution history of output displacement; (b) evolution histories of mean compliance and volume fraction.



**Fig. 5.** Optimized topologies and output displacements of the compliant inverters for various compliance constraints (a)  $C/C^0 \leq 1.2$  and  $u_{out}/u_{out}^0 = 0$ ; (b)  $C/C^0 \leq 2$  and  $u_{out}/u_{out}^0 = -2.0$ ; (c)  $C/C^0 \leq 3$  and  $u_{out}/u_{out}^0 = -6.1$ ; (d)  $C/C^0 \leq 4$  and  $u_{out}/u_{out}^0 = -10.7$ ; (e)  $C/C^0 \leq 5$  and  $u_{out}/u_{out}^0 = -14.8$ ; (f)  $C/C^0 \leq 7.5$  and  $u_{out}/u_{out}^0 = -21.3$ ; (g)  $C/C^0 \leq 10$  and  $u_{out}/u_{out}^0 = -26.3$ ; (h)  $C/C^0 \leq 20$  and  $u_{out}/u_{out}^0 = -37.1$ .

With the relative ranking of the resulting elemental sensitivity numbers,  $\hat{\alpha}_i$ , the threshold of the sensitivity number,  $\alpha_{th}$ , is determined by using the bi-section method so that the total volume of the compliant mechanism in the next iteration is equal to  $V^{i+1}$ . The design variable of the  $i$ th element is then updated by comparing its sensitivity number with the threshold as

$$x_i = \begin{cases} \min(x_i + \Delta x_i, 1) & \text{when } \hat{\alpha}_i \geq \alpha_{th} \\ \max(x_i - \Delta x_i, x_{min}) & \text{when } \hat{\alpha}_i < \alpha_{th} \end{cases} \quad (21)$$

In a summary, the BESO optimization iteration is briefly outlined as follows:

- Step 1: Assign the design domain, boundary conditions and loads for both the input dummy load case (Fig. 1b) and the output dummy load case (Fig. 1c).
- Step 2: Carry out finite element analysis (FEA) for both dummy load cases and output the displacement fields  $\{u_1\}$  and  $\{u_2\}$ .
- Step 3: Calculate the sensitivities of the objective function and the compliance constraint and determine the Lagrange multiplier  $\lambda$ .
- Step 4: Calculate elemental sensitivity numbers with Eq. (17), then modified its value with Eqs. (18) and (20).
- Step 5: Update the design variables according to Eq. (21).
- Step 6: Repeat Steps 2–5 until the objective function is convergent and both the volume constraint and the compliance constraint are satisfied.

It can see that the proposed BESO method is very simple comparing with other topology optimization algorithms and can be

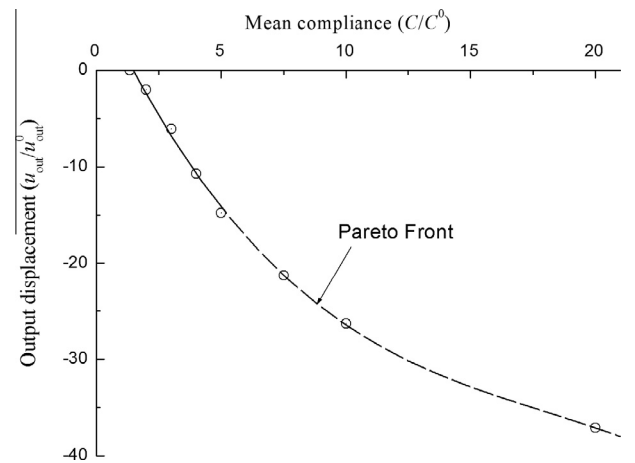


**Fig. 6.** Relationship between the output displacement and mean compliance of optimized compliant mechanisms.

easily implemented as a “post-processor” to commercial FEA software packages such as ABAQUS in this paper.

## 4. Numerical examples and discussion

### 4.1. Example 1: 2D compliant inverter

In this example, the design domain is  $120 \mu\text{m} \times 120 \mu\text{m}$  as shown in Fig. 2 which is discretized with  $120 \times 120$  4-node quadrilateral elements. It is fixed at the upper and the lower corners of



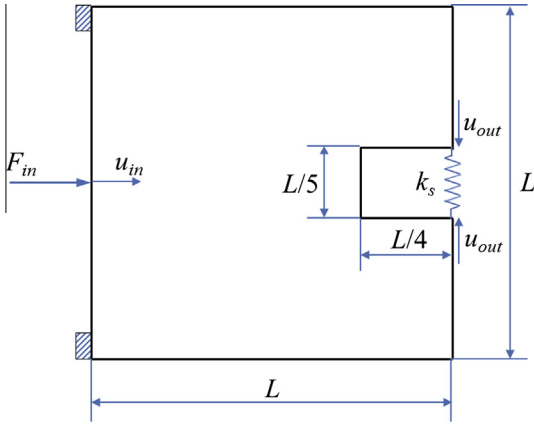


Fig. 7. Design domain and boundary conditions of the compliant gripper.

the left edge. An input force  $F_{in} = 1 \mu\text{N}$  to the right is applied at the center point of the left edge. The output port at the center point of the right edge is expected to produce a horizontal displacement,  $u_{out}$  to the left. The material properties are assumed to be Young's modulus  $E = 1 \text{ MPa}$  and Poisson's ratio  $\nu = 0.3$ . An artificial spring with stiffness  $k_s = 0.01 \mu\text{N}/\mu\text{m}$  is attached at the output port to simulate the resistance from the work-piece.

BESO starts from the initial full design with the mean compliance  $C^0$  and the output displacement  $u_{out}^0$ . In the following discussion, both the mean compliance  $C$  and the output displacement  $u_{out}$

are normalized by  $C^0$  and  $u_{out}^0$ . The volume fraction of the final design is limited to be 30% of the full design domain and the compliance constraint is set to be  $C/C^0 \leq 5$ . The used BESO parameters are evolution rate  $ER = 1\%$  and filter radius  $r_{min} = 3 \mu\text{m}$ . Fig. 3 shows the evolution history of the topology. It can be seen that there are some gray areas in the intermediate topologies which are similar to that from the other density-based optimization methods [10] due to the existence of a number of intermediate density values. With the help of these intermediate density values, stable hinge regions are formed in the final design as shown in Fig. 3(f). However, unlike other density-based optimization methods with continuous design variables, BESO utilizes discrete design variables so that possible local optimum can be easily avoided and the solution is quickly convergent to an almost black and white design. Fig. 4 shows the evolution histories of the output displacement, mean compliance and volume fraction. It can be seen that the magnitude of the output displacement gradually increases to its negative maximum value until both the volume and compliance constraints are stably satisfied. The convergent solution is achieved with 208 iterations under the convergence factor of 0.1% for both the output displacement and the mean compliance.

To demonstrate the effect of the compliance constraint on the optimized design, we apply the compliance constraint  $C/C^0 \leq 1.2, 2, 3, 4, 5, 7.5, 10, 20$  respectively. The optimized topologies for eight different cases are shown in Fig. 5. With a very small value of the compliance constraint such as  $C/C^0 \leq 1.2$ , the resulting topology is the same to that of the traditional stiffness optimization [20] resulting with the mean compliance  $C/C^0 = 1.34$ . Obviously, it is

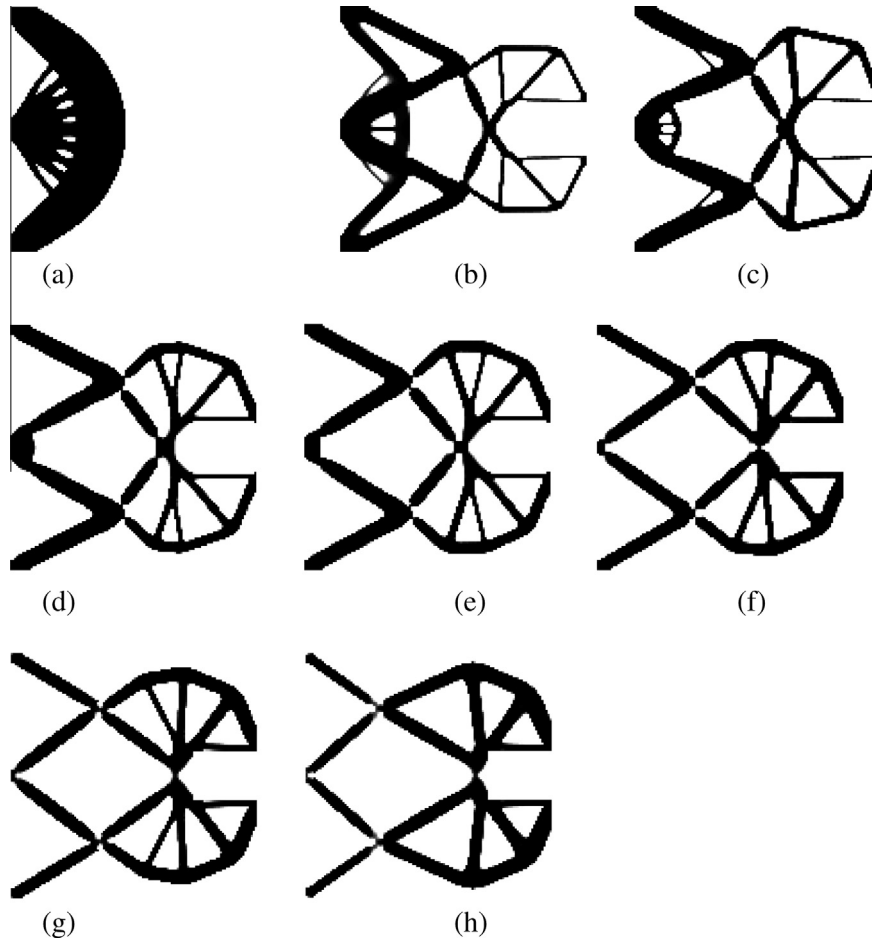


Fig. 8. Optimized topologies and output displacements of the compliant grippers for various compliance constraints (a)  $C/C^0 \leq 1.2$  and  $u_{out}/u_{out}^0 = 0$ ; (b)  $C/C^0 \leq 2$  and  $u_{out}/u_{out}^0 = -13.8$ ; (c)  $C/C^0 \leq 3$  and  $u_{out}/u_{out}^0 = -40.1$ ; (d)  $C/C^0 \leq 4$  and  $u_{out}/u_{out}^0 = -65.6$ ; (e)  $C/C^0 \leq 5$  and  $u_{out}/u_{out}^0 = -86.6$ ; (f)  $C/C^0 \leq 7.5$  and  $u_{out}/u_{out}^0 = -132.5$ ; (g)  $C/C^0 \leq 10$  and  $u_{out}/u_{out}^0 = -152.1$ ; (h)  $C/C^0 \leq 20$  and  $u_{out}/u_{out}^0 = -250.6$ .

impossible to satisfy such a low compliance constraint which is less than 1.34 and BESO therefore would minimize the mean compliance only by automatically applying  $w = 0$  in the Eq. (14). With a larger compliance constraint, BESO would maximize the output displacement and minimize the mean compliance simultaneously through gradually adjusting the value of  $w$ , so as to satisfy the specified compliance constraint. Through the observation, the optimized topologies are free of hinges for the cases with  $C/C^0 \leq 2, 3$  and 4. With the increase of the compliance constraint, the optimized topologies show numerous hinge regions which lie along the force path from the mechanism input port to the output port. Such hinge regions would favourably increase the flexibility of compliant mechanisms to efficiently transferring the energy/motion from the input port to the output port. However these hinge regions would greatly decreases the stiffness of the compliant mechanism apart from the existing difficulties in manufacturing.

As mentioned above, the design of compliant mechanism is inherently a multi-objective optimization problem. The resulting output displacements  $u_{out}/u_{out}^0$  are plotted against the values of mean compliances in Fig. 6 which shows the Pareto front with a convex curve. Generally, the magnitude of the output displacement increases with the increase of the compliance constraint. The design of compliant mechanisms is therefore a matter of making a trade-off decision from a set of compromising solutions. The solid line shown in Fig. 6 gives the possible range that the optimized topologies are free of hinges. In other words, the problematic hinges can be effectively eliminated by adopting a low compliance constraint. Compared with the approach for eliminating hinges by introducing the input-restrained compliance [30,35], the current approach compromises the output displacement with the improved load-carrying capacity of the compliant mechanism rather than that of the input-restrained structure.

#### 4.2. Example 2: 2D compliant gripper

The design domain and boundary conditions of example 2 are shown in Fig. 7 with  $L = 120 \mu\text{m}$ ,  $k_s = 0.01 \mu\text{N}/\mu\text{m}$  and  $F_{in} = 1 \mu\text{N}$ . The material properties are assumed to be Young's modulus  $E = 1 \text{ MPa}$  and Poisson's ratio  $\nu = 0.3$ . The vertical displacement,  $u_{out}$  at the output port will be maximized to grip the work-piece firmly. The BESO parameters used are evolution rate  $ER = 1\%$ , filter radius  $r_{min} = 3 \mu\text{m}$ . The objective volume fraction is to set to be 30% of the full design domain. The design domain is discretized by 4-node quadrilateral elements with the uniform sizes  $1 \mu\text{m} \times 1 \mu\text{m}$ .

BESO starts from the full design and the resulting optimized topologies are shown in Fig. 8 for various compliance constraints. When the compliance constraint  $C/C^0 \leq 1.2$ , the optimized design is the same to that of the traditional stiffness optimization. For  $C/C^0 \leq 2$ , the optimized topology show that most of materials are distributed near the input port and no hinges has been formed due to the low value of the compliance constraint. As the compliance constraint increases, more and more materials are shifted from where close to the input port to where close to the output port. The middle connections become narrower and narrower, and clear hinge regions are formed when the compliance constraint  $C/C^0 \leq 4$  by the inspection. With the further increase of the compliance constraint, the hinge regions become even clear as shown in Fig. 8. It is also observed that the hinges are located at the output port side for  $C/C^0 \leq 4, 5$  and 7.5, exactly at the connections for  $C/C^0 \leq 10$  and at the input port side for  $C/C^0 \leq 20$ . For  $C/C^0 \leq 20$ , the hinge regions are totally formed by gray areas which also demonstrates the importance of intermediate density values.

The above examples with  $k_s = 0.01 \mu\text{N}/\mu\text{m}$  show that hinge-free optimized designs can be obtained only when the compliance constraint is less than 3. It is necessary to examine the effect of the

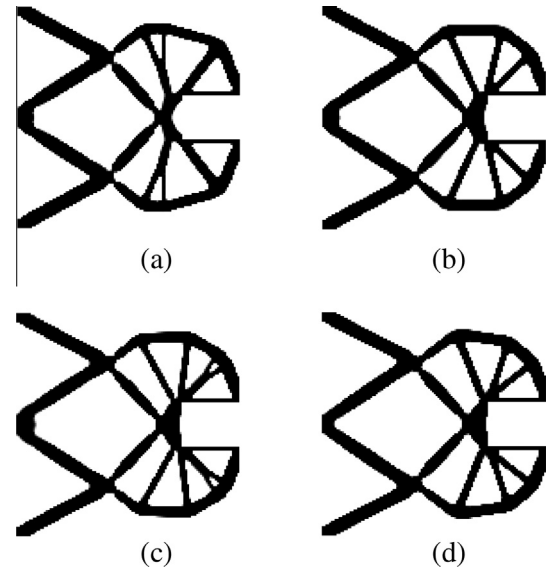


Fig. 9. Optimized topologies of the compliant grippers for various stiffness of the spring (a)  $k_s = 0.03$ ; (b)  $k_s = 0.1$ ; (c)  $k_s = 1$ ; (d)  $k_s = 10$ .

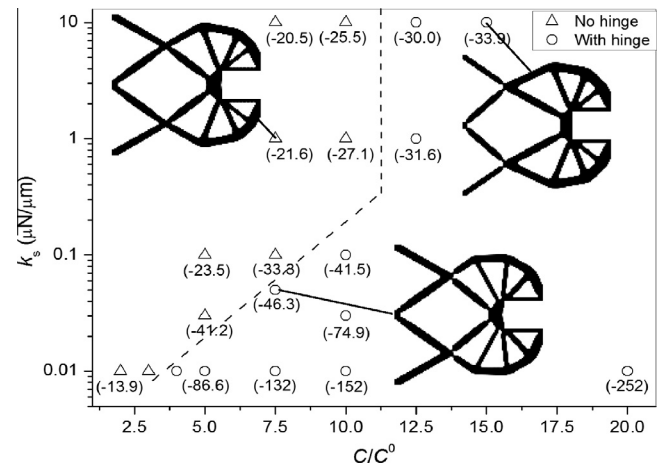


Fig. 10. Optimized designs with hinges or without hinges under various compliance constraints and stiffness of the spring (corresponding output displacement  $u_{out}/u_{out}^0$  is shown with the value in the brackets).

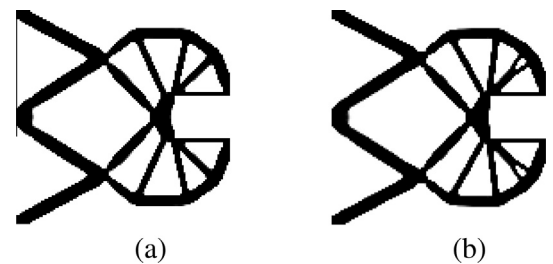


Fig. 11. Optimized topologies of the compliant gripper with soft materials (a)  $E = 0.1$ ; (b)  $E = 0.01$ .

stiffness of the work-piece on the optimized topology. Fig. 9 shows the optimized designs by imposing the constraint  $C/C^0 \leq 5$  but for  $k_s = 0.03 \mu\text{N}/\mu\text{m}$ ,  $0.1 \mu\text{N}/\mu\text{m}$ ,  $1 \mu\text{N}/\mu\text{m}$  and  $10 \mu\text{N}/\mu\text{m}$  respectively. It can be seen that these optimized topologies have no significant difference from the optimized topology for  $k_s = 0.01 \mu\text{N}/\mu\text{m}$  except that these optimized topologies are hinge-free. The connections between the input port and the output port become stronger and



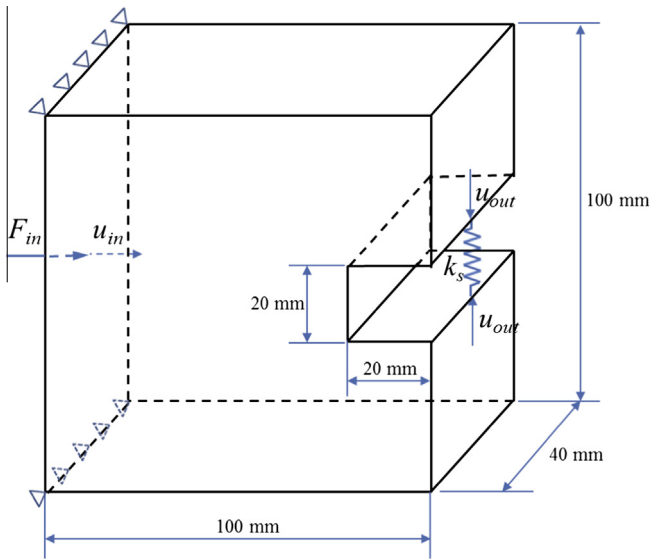


Fig. 12. Design domain and boundary conditions of a 3D compliant gripper.

stronger with the increase of the stiffness of the spring. The set of design computation results presented in Fig. 10 is intended to identify the region of free-hinge mechanism designs by considering the effects of  $k_s$  and imposed compliance constraint. It can be seen that it is only possible to obtain hinge-free compliant mechanisms when the compliance constraint is less or equal than about 10. Even when the compliance constraint is less than 10, hinge regions still occur at the output port side of the connections as shown by the inset for a spring with low stiffness. Such hinges can be effectively eliminated by increasing the stiffness of the spring which consequently increases the stiffness at the output

part side. However, when the compliance constraint is larger than 10, hinge regions normally occur at the input port side of the connections as shown by the inset. Increasing the stiffness of the spring has little effect on the stiffness of the input port side and therefore fails to preclude the formation of these hinges.

The above results indicate that it is difficult to design a hinge-free compliant mechanism for a soft work-piece such as  $k_s = 0.01$ . In order to obtain a hinge-free compliant mechanism for a soft work-piece, we may select a soft material for the compliant mechanism. Numerical examples in Fig. 11 demonstrate that hinge-free optimized mechanisms for  $k_s = 0.01$  and  $C/C^0 \leq 5$  can still be achieved by using a soft material such as  $E = 0.1$  MPa or 0.01 MPa. It also indicates that selecting materials is very important factor for designing compliant mechanisms which is totally different from the stiffness optimization in which the optimized topology is independent from the stiffness of the material [10].

#### 4.3. Example 3: 3D compliant gripper

The current BESO algorithm can be easily extended for 3D cases. Fig. 12 shows the design domain and boundary conditions of a 3D gripper mechanism. The force  $F_{in} = 1$  kN is applied to the input port located at the center of the left face. A spring with  $k_s = 1$  kN/mm is attached to the output port as shown in Fig. 11. The design domain is discretized with 8-node brick elements with the uniform sizes  $1 \text{ mm} \times 1 \text{ mm} \times 1 \text{ mm}$ . Here, the material considered is nylon with Young's modulus  $E = 3$  GPa and Poisson's ratio  $\nu = 0.4$ . The BESO parameters are evolution rate  $ER = 1\%$  and filter radius  $r_{min} = 3$  mm. The objective volume fraction is set to be 10% of the full design domain.

The optimized designs are shown in Fig. 13 when the compliance constraint  $C/C^0 \leq 2, 3$  and 5 is adopted respectively. The resulting optimized topologies for these three cases are different due to the

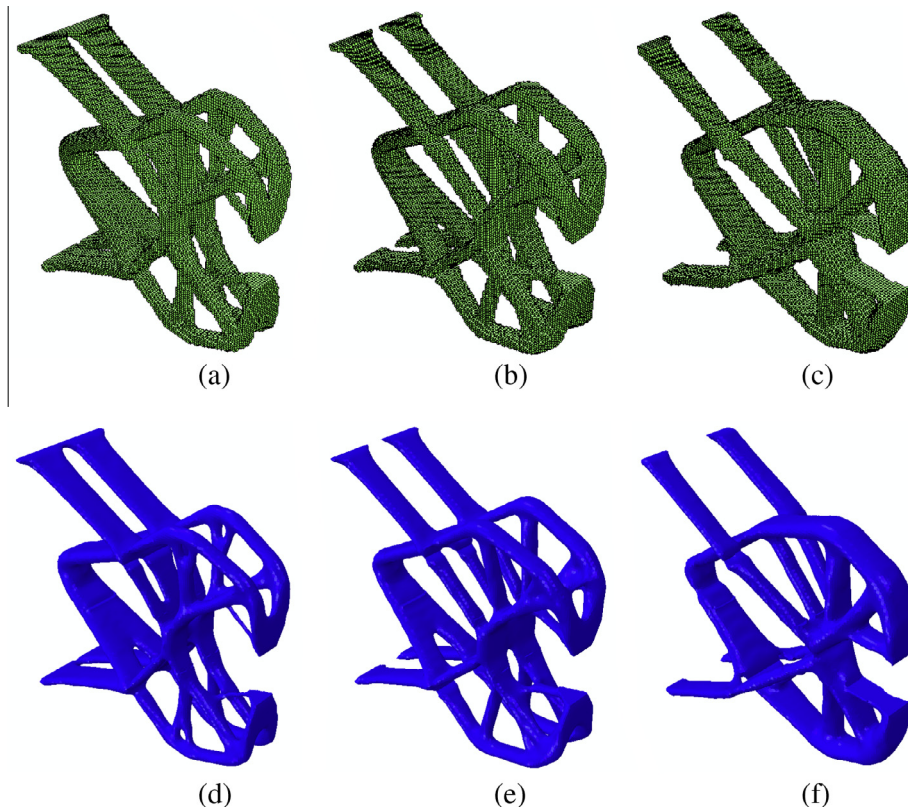


Fig. 13. Optimized topologies and CAD models of 3D compliant grippers with various compliance constraints: (a)  $C/C^0 \leq 2$  and  $u_{out}/u_{out}^0 = -236$ ; (b)  $C/C^0 \leq 3$  and  $u_{out}/u_{out}^0 = -412$ ; (c)  $C/C^0 \leq 5$  and  $u_{out}/u_{out}^0 = -688$ ; (d) CAD model for (a); (e) CAD model for (b); (f) CAD model for (c).

different compliance constraint. The corresponding output displacements  $u_{out}/u_{out}^0$  are –236, –412 and –688 respectively. Similar to 2D cases, the magnitude of the output displacement increases with the increase of the compliance constraint. The smooth CAD models for these optimized topologies are also given in Fig. 13.

## 5. Conclusion

This paper has proposed a new and simple BESO method for topology optimization of compliant mechanisms by maximizing the flexibility subject to the mean compliance and volume constraints. The compliance constraint is imposed on the optimization algorithm by introducing a Lagrange multiplier. Based on the derived sensitivity numbers, the discrete design variables are gradually updated until a convergent solution is achieved.

Using the proposed BESO method, a set of optimized designs with and without hinges has been obtained by altering the desired structural stiffness of compliant mechanisms. The flexibility of the optimized compliant mechanism generally increases with increasing the compliance constraint, so that the resulting design has the improved capacity of transferring the energy/motion from the input port to the output port. However, such an optimized compliant mechanism may have low stiffness to resist the external forces and also contain hinge regions which are difficult to manufacture especially for a micro system. To achieve a hinge-free compliant mechanism, it is recommended that the flexibility of the compliant mechanism can be optimized by specifying a low compliance constraint or increasing the stiffness of the work-piece. For an extreme soft work-piece, selecting a soft material for compliant mechanisms can also preclude the formation of hinge regions during the optimization process.

## References

- [1] Howell LL. Compliant mechanisms. New York: John Wiley & Sons; 2001.
- [2] Howell LL, Midha A. A loop-closer theory for the analysis and synthesis of compliant mechanisms. *J Mech Des* 1996;118:121–5.
- [3] Pedersen CBW, Buhl T, Sigmund O. Topology synthesis of large-displacement compliant mechanisms. *Int J Numer Meth Eng* 2001;50:2683–705.
- [4] Saxena A, Ananthasuresh GK. Topology design of compliant mechanisms with strength consideration. *Mech Struct Mech* 2003;29(2):199–221.
- [5] Sigmund O. On the design of compliant mechanisms using topology optimization. *Mech Struct Mech* 1997;25(4):495–526.
- [6] Luo Z, Tong L, Wang MY, Wang S. Shape and topology optimization of compliant mechanisms using a parameterization level set method. *J Comput Phys* 2007;227:680–705.
- [7] Bendsoe MP, Kikuchi N. Generating optimal topologies in structural design using a homogenization method. *Comput Meth Appl Mech Eng* 1988;71:197–224.
- [8] Bendsoe MP. Optimal shape design as a material distribution problem. *Struct Opt* 1989;1:193–202.
- [9] Zhou M, Rozvany GIN. DCOC – an optimality criteria method for large systems, Part I: Theory. *Struct Opt* 1992;5:12–25.
- [10] Bendsoe MP, Sigmund O. Topology optimization: theory, methods and applications. Berlin: Springer-Verlag; 2003.
- [11] Sethian JA, Wiegmann A. Structural boundary design via level set and immersed interface methods. *J Comput Phys* 2000;163(2):489–528.
- [12] Wang MY, Wang XM, Guo DM. A level set method for structural topology optimization. *Comput Meth Appl Mech Eng* 2003;192:227–46.
- [13] Xie YM, Steven GP. A simple evolutionary procedure for structural optimization. *Comput Struct* 1993;49:885–96.
- [14] Xie YM, Steven GP. Evolutionary structural optimization. London: Springer; 1997.
- [15] Rong JH, Tang ZL, Xie YM, Li FY. Topological optimization design of structures under random excitations using SQP method. *Eng Struct* 2013;56:2098–106.
- [16] Kaveh A, Hassani B, Shojaei S, Tavakkoli SM. Structural topology optimization using ant colony methodology. *Eng Struct* 2008;30(9):2559–65.
- [17] Tovar A, Khandelwal K. Topology optimization for minimum compliance using a control strategy. *Eng Struct* 2013;48:674–82.
- [18] Querin OM, Steven GP, Xie YM. Evolutionary structural optimization (ESO) using a bi-directional algorithm. *Eng Comp* 1998;15:1031–48.
- [19] Huang X, Xie YM. Convergent and mesh-independent solutions for the bi-directional evolutionary structural optimization method. *Finite Elem Anal Des* 2007;43(14):1039–49.
- [20] Huang X, Xie YM. Evolutionary topology optimization of continuum structures: methods and applications. Chichester: John Wiley & Sons; 2010.
- [21] Huang X, Xie YM. Bi-directional evolutionary topology optimization of continuum structures with one or multiple materials. *Comp Mech* 2009;43(3):393–401.
- [22] Huang X, Zuo ZH, Xie YM. Evolutionary topology optimization of vibrating continuum structures for natural frequencies. *Comp Struct* 2010;88:357–64.
- [23] Huang X, Xie YM, Lu G. Topology optimization of energy absorption structures. *Inter J Crash* 2007;12(6):663–75.
- [24] Huang X, Xie YM. Topology optimization of nonlinear structures under displacement loading. *Eng Struct* 2008;30(7):2057–68.
- [25] Ghabraie K, Chan R, Huang X, Xie YM. Shape optimization of metallic yielding devices for passive mitigation of seismic energy. *Eng Struct* 2010;32(8):2258–67.
- [26] Lau GK, Du H, Lim MK. Use of functional specifications as objective functions in topology optimization of compliant mechanism. *Comput Meth Appl Mech Eng* 2001;190:4421–33.
- [27] Larsen U, Sigmund O, Bouwstra S. Design and fabrication of compliant micro-mechanisms and structures with negative Poisson's ratio. *J Microelectromech Syst* 1997;6:99–106.
- [28] Burns TE, Tortorelli DA. An element removal and reintroduction strategy for the topology optimization of structures and compliant mechanisms. *Int J Numer Meth Eng* 2003;57:1413–30.
- [29] Shield RT, Prager W. Optimal structural design for given deflection. *J Appl Math Phys* 1970;21:513–23.
- [30] Rahmatalla S, Swan CC. Sparse monolithic compliant mechanisms using continuum structural topology optimization. *Int J Numer Meth Eng* 2005;62:1579–605.
- [31] Ansola R et al. 3D compliant mechanisms synthesis by a finite element addition procedure. *Finite Elem Anal Des* 2010;46(9):760–9.
- [32] Ansola R et al. A simple evolutionary topology optimization procedure for compliant mechanism design. *Finite Elem Anal Des* 2007;44(1–2):53–62.
- [33] Lin J, Luo Z, Tong L. A new multi-objective programming scheme for topology optimization of compliant mechanisms. *Struct Multidis Opt* 2010;40:241–55.
- [34] Poulsen TA. Topology optimization in wavelet space. *Int J Numer Meth Eng* 2002;57:741–60.
- [35] Yoon GH et al. Hinge-free topology optimization with embedded translation-invariant differentiable wavelet shrinkage. *Struct Multidis Opt* 2004;27(3):139–50.
- [36] Poulsen TA. A new scheme for imposing a minimum length scale in topology optimization. *Int J Numer Meth Eng* 2003;57:741–60.
- [37] Sigmund O. Morphology-based black and white filters for topology optimization. *Struct Multidis Opt* 2007;33:401–24.
- [38] Frecker MI et al. Topological synthesis of compliant mechanisms using multi-criteria optimization. *J Mech Des* 1997;119:238–45.
- [39] Zhu B, Zhang X, Wang N. Topology optimization of hinge-free compliant mechanisms with multiple outputs using level set method. *Struct Multidis Opt* 2013;47:659–72.
- [40] Haug EJ, Choi KK, Komkov V. Design sensitivity analysis of structural systems. Orlando: Academic Press; 1986.
- [41] Huang X, Xie YM. Evolutionary topology optimization of continuum structures with an additional displacement constraint. *Struct Multidis Opt* 2010;40:409–16.